Mangafodipir trisodium-enhanced MR imaging of hepatocellular carcinoma: correlation with histologic characteristics

Joo Hee Kim

The Graduate School

Yonsei University

Department of Medicine

Mangafodipir trisodium-enhanced MR imaging of hepatocellular carcinoma: correlation with histologic characteristics

Directed by Professor Myeong-Jin Kim

The Doctoral Dissertation submitted to the Department of Medicine and the Graduate School of Yonsei University in partial fulfillment of the requirements for the degree of Doctor of Philosophy

Joo Hee Kim

December 2005

This certifies that the Doctoral Dissertation of

Joo Hee Kim is approved.

Myeong-Jin Kim : Thesis Supervisor

Jong Tae Lee : Thesis Committee Member

Byong Ro Kim : Thesis Committee Member

Jae Bock Chung : Thesis Committee Member

Young Nyun Park : Thesis Committee Member

The Graduate School

Yonsei University

December 2005

ACKNOWLEDGEMENTS

There have been a number of people without whom this thesis could not be completed. I would like to express my deepest gratitude to my thesis supervisor and mentor Professor Myeong-Jin Kim. He always gave many academic guidance and discipline as a professor not to be downed to an error, and sometimes gave me a big smile and encouragement as a senior whenever I suffer hardship during my work.

I would like to thank Dr. Jong Tae Lee, Dr. Byong Ro Kim, Dr. Jae Bock Chung and especially Dr. Young Nyun Park for their perceptive comments, and ongoing and persistent efforts to help me make good thesis.

I would like to express my infinite gratitude to my dear husband who gave me unchanged applause and encouragement. I am deeply indebted to my parents and parents-in-law, who always provided a solid foundation for me to spread my wings.

December 2005

Joo Hee Kim

TABLE OF CONTENTS

LIST OF FIGURES

LIST OF TABLES

ABSTRACT

Mangafodipir trisodium-enhanced MR imaging of hepatocellular carcinoma: correlation with histologic characteristics

Joo Hee Kim

Department of Medicine
The Graduate Scholl, Yonsei University

(Directed by Professor **Myeong-Jin Kim)**

Purpose: To define histopathologic factors related with the degree of mangafodipir trisodium (MnDPDP) uptake in hepatocellular carcinomas (HCCs) on magnetic resonance (MR) imaging.

Materials and Methods: In-phase and opposed-phase gradient echo (GRE) MR images were obtained preoperatively in 37 patients with 38 HCCs before and 15 – 30 min after intravenous injection of MnDPDP. Subjective ratings of the enhancement degree, the signal-to-noise ratio (SNR) of the lesion and the liver before and after MnDPDP enhancement and the signal enhancement ratios (ER, %) were all correlated with the

histopathologic factors; these included the nuclear grade, the size of tumor, growth type, presence of capsule, histologic type, cell type, the cell density ratio of the tumor to the adjacent parenchyma (cellular compactness), the percentage of the immunopositive areas on immunostaining for monoclonal hepatocyte antibody (Hep Par 1), cytokeratin 7 (CK7), and cytokeratin 19 (CK19).

Results: Compared to the precontrast MR images, the mean SNR of HCCs increased from 59.6 to 95.0 (ER of HCC = 59.5 %) on the MnDPDP-enhanced MR images, while the mean SNR of the liver increased from 75.1 to 108.7 (ER of the liver = 45.2 %). In 34 HCCs, 8 showed mild enhancement, 11 showed moderate enhancement, and 15 showed strong enhancement. There was no visually perceptible enhancement in the remaining 4 HCCs (10.3 %). As MnDPDP enhancement increased, the cell density ratio also increased ($p < .05$). There was strong correlation between the degree of MnDPDP enhancement and Hep Par 1 positivity ($p < .005$). There were no significant correlations between the degree of MnDPDP enhancement and the nuclear grade, size, growth type, presence of capsule, cell type, histologic type, CK7, or CK19.

Conclusion: Initial delayed uptake of MnDPDP in HCCs was correlated with

hepatocyte antibody expression and cellular density. The histologic differentiation of HCCs was not directly correlated with the degree of enhancement on MnDPDP-enhanced MR imaging.

Key words: **Hepatocellular carcinoma, Magnetic resonance imaging, MR contrast agent, mangafodipir trisodium**

Mangafodipir trisodium-enhanced MR imaging of hepatocellular carcinoma: correlation with histologic characteristics

Joo Hee Kim

Department of Medicine
The Graduate Scholl, Yonsei University

(Directed by Professor **Myeong-Jin Kim)**

I. Introduction

Magnetic resonance (MR) imaging of the liver is useful in the detection and characterization of focal hepatic lesions. Further improvements in MR imaging could be achieved by extracellular MR contrast, which was non-tissue-specific[1]. However, this most widely-used extracellular MR contrast agents, gadolinium-chelates, behave the same way as iodinized CT contrast agents with regard to contrast distribution and enhancement patterns for hepatic imaging. Thus, differentiation between hepatocellular and non-hepatocellular tumors or between benign and malignant hepatic tumors remains difficult in some cases. In order to obtain this additional benefit of hepatic MR imaging,

the need for tissue-specific contrast agents has emerged.

Mangafodipir trisodium (Manganese-dipyridoxal diphosphate, MnDPDP) is an anionic manganese chelate that dissociates rapidly following administration, yielding a free Mn^{++} ion. The free Mn^{++} is taken up by active hepatocytes and excreted through the biliary system[2, 3]. It is well known that not only normal hepatocytes, but also parts of hepatocyte-derived tumor cells, take up MnDPDP[4]. Thus, MnDPDP-enhanced liver MRI has been shown to be valuable for the detection and characterization of hepatic tumors[5-7] and to be useful for distinguishing between hepatocellular and non-hepatocellular tumors[7-11]. However, it is still uncertain which factors influence the degree of enhancement of HCCs during the initial delayed phase of MnDPDP-enhancing images. Some authors reported that the degree of tumor enhancement by MnDPDP correlated with the histologic grades of the HCCs[12-14], but this assertion was controversial by other investigators[10]. These previous studies had several limitations: insufficient materials, lack of complete surgical correlation, lopsided histologic differentiation, or lack of statistical significance.

Although MnDPDP can distinguish between hepatocellular and non-hepatocellular tumors, MnDPDP has not been used effectively in making differentiation the different types of hepatocellular tumors. Evidence suggests that there are other factors other than

tumor grade that influence early enhancement on MnDPDP-enhanced MR imaging. Finding determinants of the patterns and degrees of MnDPDP uptake may assist in the detection and characterization of hepatocyte-derived tumors, and also suggest another prognostic factor for HCC. The aim of this study was to define histopathologic factors related to the degree of MnDPDP uptake in HCCs on MR imaging.

II. Materials and Methods

1. Patients

MnDPDP-enhanced hepatic MR examinations were performed in 74 patients as preoperative assessment of HCC at the Severance Hospital. Among them, a total of 37 patients with 38 HCCs underwent hepatic resection: these patients were enrolled in this study (24 male and 13 female; mean age, 53 years; age range, 33–76 years). The criteria of exclusion were cases of non-surgical treatment (n=24), a history of prior trans-arterial chemo-embolization (n=6), prior use of other MR contrast agents such as gadolinium-chelates or superparamagnetic iron oxide (n=5), and mixed-type malignancy (hepatocellular and cholangiocellular carcinoma) (n=2). All the lesions had complete surgical pathology.

2. MR Imaging

All MR imaging was performed on 1.5-T MR scanners (Signa Horizon; General Electric Medical Systems, Milwaukee, WI) using phased-array multicoils. A rectangular field of view (FOV) of 32 × 24 to 29 × 22 cm, adjusted for each patient was held constant for all the sequences. In all patients, the unenhanced and MnDPDP-enhanced

MR images were obtained.

The pre-contrast MRI was composed of 1) a respiratory-triggered T2-weighted fast spin-echo (FSE) (effective TR range/effective TE, 3500–10900/96–105; echo train length, 12–16; two signal averages; a 256 × 256 matrix; superior and inferior spatial presaturation and chemically selective fat saturation; and a 7- to 8-mm thick slice with a 1- to 2-mm gap), 2) breath-hold T1-weighted fast multi-planar spoiled gradient recalled echo (GRE) in-phase images (150–200/4.2–4.4) and 3) out-of-phase images (120–180/1.5–2.2; 90° flip angle; one signal average; a 256 × 128 matrix; 8 mm thick slices, zero gap; interleaved), and 4) breath-hold T2-weighted single-shot half-Fourier images (single-shot FSE; effective TE, 180; a 256 × 160 matrix; and 8 mm-thick slices with a 2-mm gap).

For the MnDPDP-enhanced MRI, 5 μmol per kg of body weight (0.5 mL/kg; maximum dose, 50 mL) of MnDPDP (Teslascan®, Amersham Health, Oslo, Norway) was slowly administered intravenously by a hand injection over a 1- or 2-minute period, which was followed by a flush of 10 mL normal saline. The breath-hold T1-weighted spoiled GRE in-phase and out-of-phase images were obtained 15 minutes after the intravenous injection of MnDPDP. Pre- and post-contrast pulse sequence parameters were identical.

3. Image Analysis

For qualitative image analysis, two experienced radiologists jointly analyzed matched unenhanced and MnDPDP-enhanced MR images. Radiologists recorded the degree of the HCCs' enhancement with respect to the adjacent hepatic parenchyma. Relative signal intensity of HCCs compared with that of surrounding liver parenchyma was recorded as one of four degrees: no gross enhancement, weak enhancement, moderate enhancement (signal indicated a tumor of hepatocellular origin, but was not equivalent to the adjacent hepatic parenchyma), strong enhancement (signal equivalent to adjacent hepatic parenchyma).

For quantitative image analysis, measurement of the signal intensity of the lesions was obtained using an operator-defined region of interest (ROI). The liver parenchyma adjacent to the lesion was measured using an ROI that excluded artifacts and blood vessels. Because the distance from the surface coil may affect measured values, the ROI of the liver parenchyma adjacent to a hepatic lesion was located, so that the vertical distances from the ventral side of the surface coils to the ROIs were the same. The background noise was measured using the largest possible ROI located ventrally to the patient's abdomen in the direction of the phase-encoding gradient, in an area without phase shift artifacts.

Signal-to-noise ratios (SNR) of the liver and the lesion on unenhanced and MnDPDP-enhanced MR images were calculated with the following formulas:

SNR_{liver} = signal intensity $(SI)_{liver}$ / standard deviation of background noise (NSD)

$SNR_{tumor} = SI_{tumor} / NSD$

The signal enhancement ratios of the tumor and that of the liver were calculated with the following formula:

Signal enhancement ratio (%) = $(SNR_{post} - SNR_{pre}) / (SNR_{pre}) \times 100$

4. Pathologic Analysis

Whole specimens of HCCs were retrieved and all tissue sections were fixed in 10% buffered formaldehyde solution and paraffinized. An effort was made to perform the pathology inspection in the same area where the MRI analysis was carried out. According to the general rules for the study of primary liver cancer by the KOREAN LIVER CANCER STUDY GROUP, the histopathologic factors making influence on MnDPDP uptake were assessed for each tumor; these factors included the nuclear grade, size of the tumor, growth type, histologic type, cell type, the cell density ratio of the tumor to the adjacent parenchyma, the percentage of the immunopositive areas on immunostaining for monoclonal hepatocyte antibody (hepatocyte paraffin 1, Hep Par 1),

cytokeratin 7 (CK 7), and cytokeratin 19 (CK 19).

Using the basic hematoxylin-eosin (H&E) technique, tumor grade of the HCCs was classified according to the nuclear grading scheme by Edmondson-Steiner, as I, I+II, II, II+III, III, III+IV, and IV. We also defined grades I, I+II, and II as being well differentiated, grades II+III and III as moderately differentiated, and grade III+IV and IV as poorly differentiated. Tumor size was defined as the largest diameter of the tumor specimen. The growth type was defined as either nodular expanding, nodular with perinodular growth, multinodular-confluent, or infiltrative; histologic type was defined as either trabecular, pseudoglandular, compact, or scirrhous; cell type was defined as hepatic, clear, giant, or spindle. The encapsulation was defined as absence, partial, or complete.

Image Pro Plus 4.0 (Media Cybernetics Inc. Silver Spring, USA) software was used for image acquisition and for the counting of cell density. Three random areas were selected from each tumor and from surrounding non-neoplastic liver tissue in high-power fields (×200). Then, individual nuclei were counted per 120000 μm^2 using tools provided by Image Pro. Cell density ratio was calculated with the following formula:

Cell density ratio = mean cell density $_{tumor}$ / mean cell density $_{liver}$

Immunohistochemical staining was carried out for Hep Par 1 and biliary markers,

CK7 and CK19. A commercially available monoclonal antibody, Hep Par 1 (DAKO, Glostrup, Denmark), was used at a dilution of 1:25. The monoclonal antibodies CK7 (DAKO, Glostrup, Denmark) and CK19 (DAKO, Glostrup, Denmark) were used at dilutions of 1:50. Immunoreactivity was quantitated as the percent of area positive for each marker. Immunohistochemical reactivity was also semiquantitatively classified into four categories; - <5%, + 5–10%, ++ 10–50%, and +++ >50% of tumor cells.

5. Statistics

All collected data were analyzed using the statistical program, SPSS (version 12.0 for Windows). For statistical analysis, a chi-square test was used for nominal variables and the Kruskal-Wallis test for continuous variables to compare MnDPDP enhancement with the various histopathologic factors. The post hoc Dunnett's t-test was used to determine statistically significant differences between MnDPDP enhancement groups. All p values were two-tailed and, when less than 0.05, were considered to indicate a statistically significant difference.

III. Results

1. Qualitative and quantitative enhancement of MnDPDP

The enhancement of the lesions after MnDPDP injection was variable. The SNR of HCCs increased from 59.6 ± 15.5 to 95.0 ± 28.5 (signal enhancement ratio of the HCC = 59.5 %), while the SNR of the liver increased from 75.1 ± 21.6 to 108.7 ± 37.5 (signal enhancement ration of the liver = 45.2 %). When the signal enhancement ratio (ER) of the HCC was less than 30%, MnDPDP enhancement was not grossly perceptible and nonspecific (n=4, 10.5 %). Most HCCs had an ER of more than 30% and those were determined to be hepatocellular tumors (89.5%). HCCs with 30–45% ERs were perceived as having minimal enhancement (n=8), those with 45–70% ERs as having moderate enhancement (n=11), and those with ERs of more than 70% as having strong enhancement (n=15).

2. MnDPDP enhancement and pathomorphology of HCCs

There were 2 HCCs with grade I+II, 17 with grade II, 8 with grade II+III, 8 with grade III, and 3 with grade III+IV; there were 19 well differentiated, 16 moderately differentiated, and 3 poorly differentiated HCCs. The size of the tumors ranged from 1.3

to 11.0 cm (mean, 4.6 cm). Sixteen HCCs had nodular expanding growth patterns, 8 were of the nodular type with perinodular growth, and 14 were of the multinodular-confluent type. The histologic types consisted of 18 trabecular, 2 pseudoglandular, 1 compact, 2 scirrhous, and 15 mixed types (6 trabecular and pseudoglandular, 5 trabecular and compact, 2 trabecular and scirrhous, 2 trabecular, pseudoglandular and compact). The cell types consisted of 27 hepatic, 3 clear, and 8 mixed types (5 hepatic and clear, 2 hepatic and giant, and 1 hepatic and spindle). There were no pseudocapsules in 8 HCCs, partial pseudocapsules in 15 HCCs, and complete pseudocapsules in 15 HCCs.

Nodular expanding HCCs and nodular HCCs with perinodular growth tended to show stronger enhancement than multinodular confluent HCCs, but the differences were statistically insignificant. As far as histologic type, trabecular, the most common histologic type, showed variable MnDPDP enhancements. Compact or scirrhous histologic type HCCs showed no or minimal enhancement, but results were not statistically significant because of the small number of cases. There were no significant correlations between the degree of MnDPDP enhancement and tumor size, the presence of the capsule, or cell type.

3. MnDPDP enhancement and the histologic grades

The relationship between the degree of MnDPDP enhancement and histologic grade is shown in Table 1. In cases of the same histologic grade, HCCs showed various degrees of MnDPDP enhancement from no enhancement to strong enhancement for each grade (Figure 1–4). There was no significant correlation between the degree of MnDPDP enhancement and the histologic grade of tumors in our study ($p = 0.156$).

Table 1. Relationship between the degree of MnDPDP enhancement and histologic grade of HCC.

MnDPDP enhancement	Histologic Grade				
	G I+II	G II	G II+III	G III	G III+IV
No		1	1	1	1
Minimal	1	4	2	1	
Moderate	1	2	2	5	1
Strong		10	3	1	1

Figure 1. A 59-year-old male with grade II HCC showing no gross enhancement of MnDPDP.

Opposed-phase GRE axial images before (a) and after (b) MnDPDP administration showed a well demarcated hypointense nodule (arrows) in the lateral segment of the left hepatic lobe with no grossly perceptible enhancement, measuring 2.0cm in size. Quantitatively, the signal enhancement ratio of the tumor was 30%. A nuclear grade II trabecular HCC with multinodular confluent growth, hepatic and clear cells and no capsule was determined (c). Immunoreactivity of Hep Par 1 was totally negative (d). The cell density ratio was 0.94. CK7 (e) and CK19 (f) were also negative.

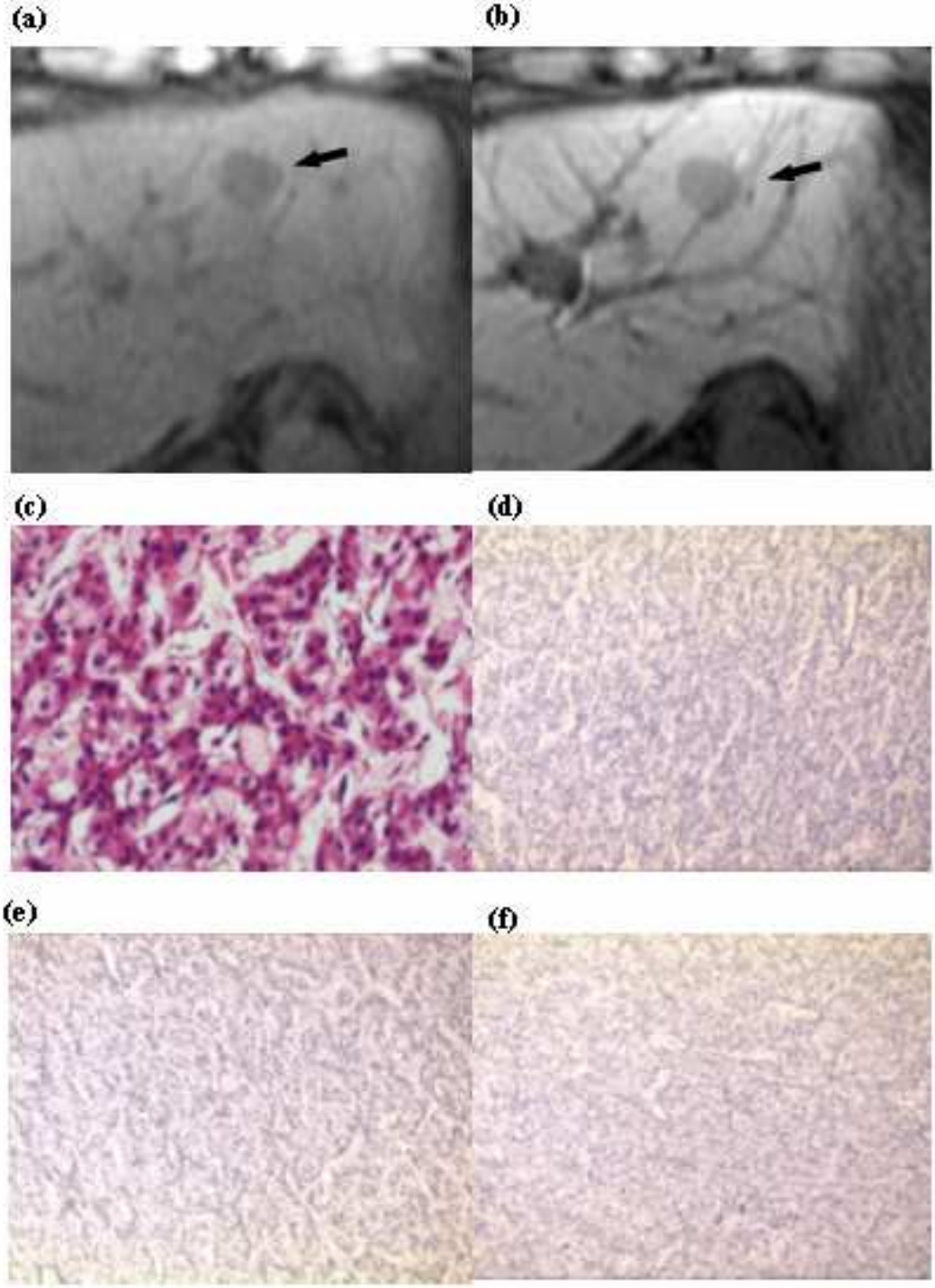

Figure 2. A 50-year-old male with grade II HCC showing mild enhancement of MnDPDP.

Opposed-phase GRE axial images before (a) and after (b) MnDPDP administration showed a 2.2cm-sized hypointense nodule (arrows) in the lateral segment of the left hepatic lobe with faint enhancement at the periphery. Quantitatively, the signal enhancement ratio of the tumor was 36%. A nuclear grade II trabecular HCC with multinodular confluent growth, hepatic cells and no capsule was determined (c). Immunoreactivity of Hep Par 1 was positive (arrowheads) in about 40% of areas (d). The cell density ratio was 1.72. CK7 was (+) (e) and CK19 was negative (f).

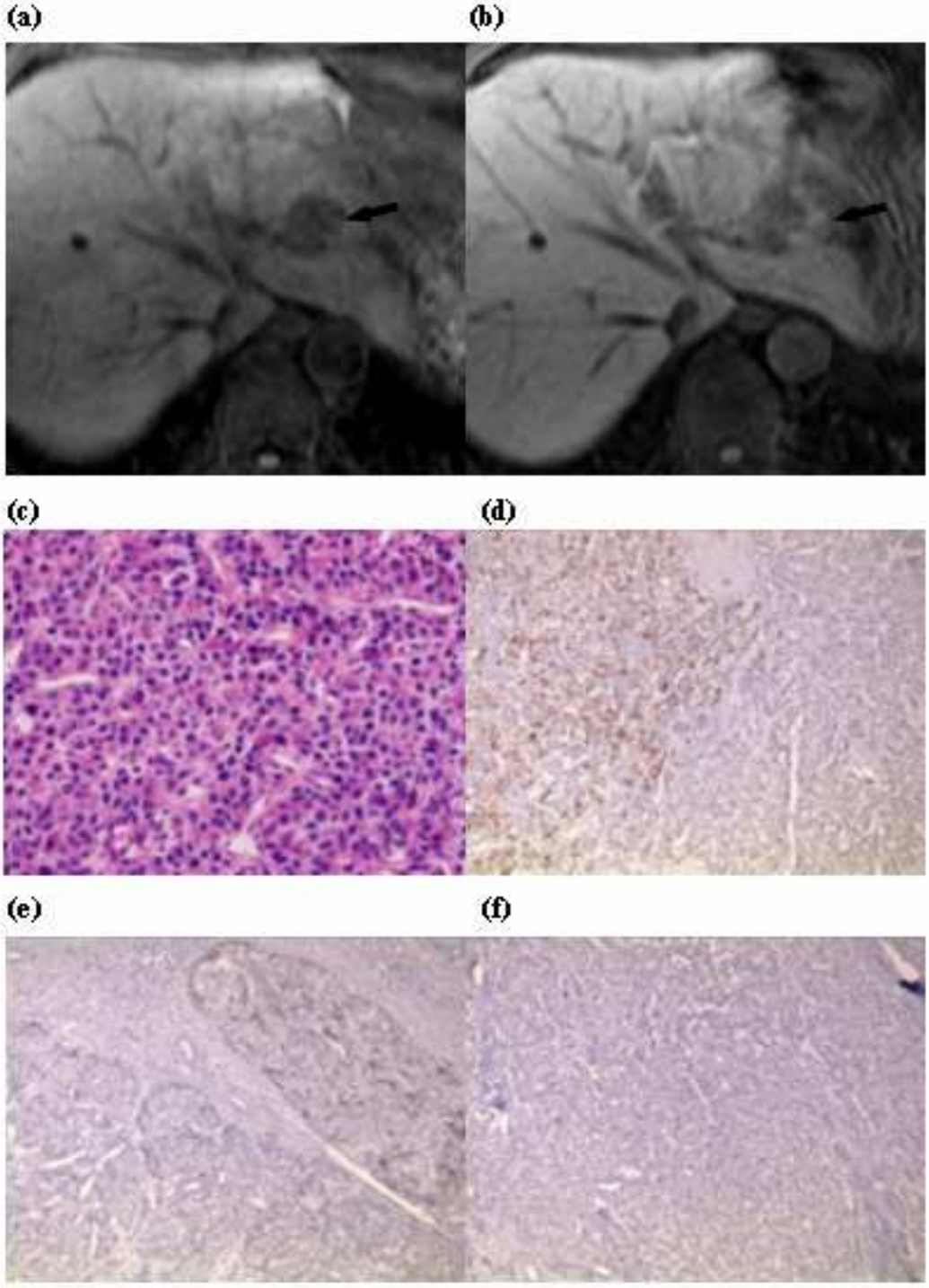

Figure 3. A 76-year-old male with grade II HCC showing moderate enhancement of MnDPDP.

In-phase GRE axial images before (a) and after (b) MnDPDP administration showed a 8cm-sized mass (arrows) in the lateral segment of the left hepatic lobe with moderate enhancement. Quantitatively, signal enhancement ratio of the tumor was 56%. A nuclear grade II trabecular and pseudoglandular HCC with nodular growth, hepatic cells and a partial capsule was proven (c). Immunoreactivity of Hep Par 1 was strongly positive in about 80% of areas (d). The cell density ratio was 2.40. CK7 was (++) (e) and CK19 was (+++) (f).

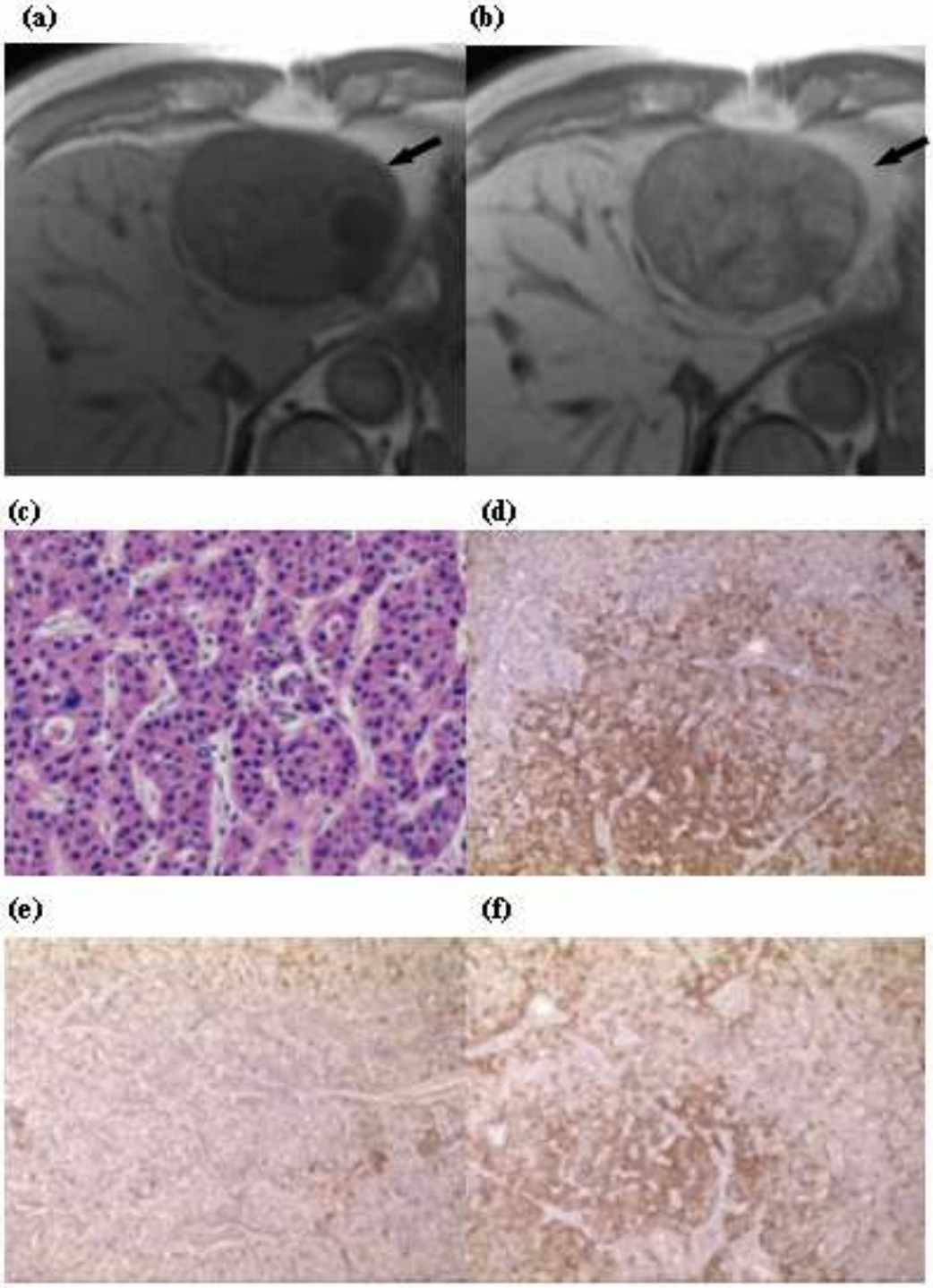

Figure 4. A 35-year-old female with grade II HCC showing strong enhancement of MnDPDP.

In-phase GRE axial images before (a) and after (b) MnDPDP administration showed a 3.5cm-sized mass (arrows) in the lateral segment of the left hepatic lobe with strong enhancement. Quantitatively, signal enhancement ratio of the tumor was 91%. A nuclear grade II trabecular HCC with nodular growth, hepatic cells and a complete capsule was proven (c). Immunoreactivity of Hep Par 1 was strongly positive in whole areas (d). The cell density ratio was 5.07. CK7 was negative (e) and CK19 was (+++) (f).

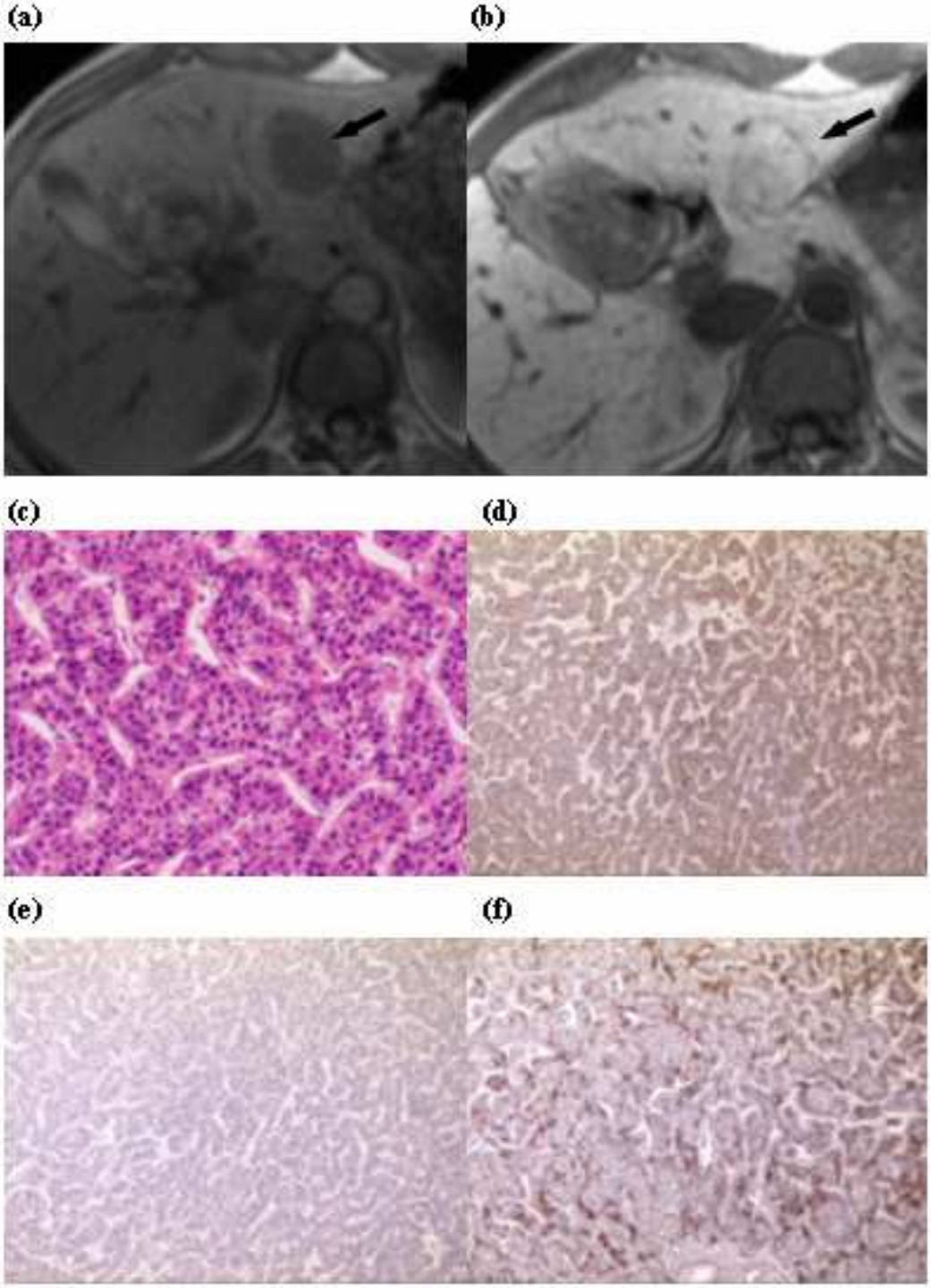

4. MnDPDP enhancement and the cell density ratio

The ratios of the cell densities of the HCC to liver tissue are shown in Figure 5. As MnDPDP enhancement increased, the cell density ratio of the tumor to non-tumor also increased significantly ($p = 0.043$).

Figure 5. Relationship between the degree of MnDPDP enhancement and the tumor to non-tumor cell density ratio.

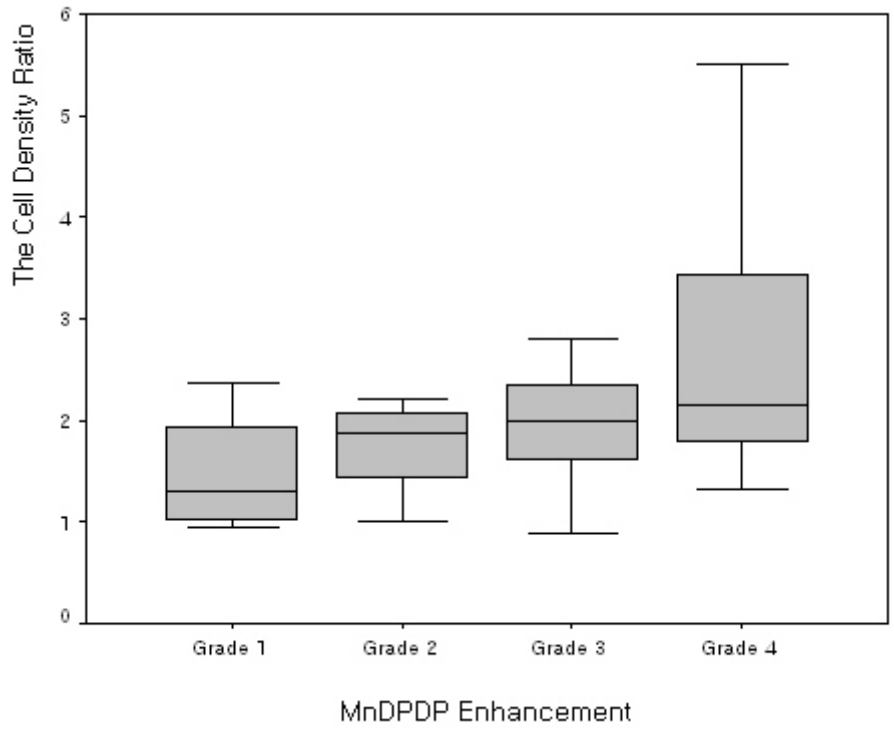

5. MnDPDP enhancement and immunohistologic evaluation

The relationship between the degree of MnDPDP enhancement and Hep Par 1 positivity is shown in Table 2. There were 6 cases of Hep Par 1 negativity (15.8%). Half of the HCCs had strong positivity on immunohistochemical staining for Hep Par 1. There was strong correlation between the degree of MnDPDP enhancement and Hep Par 1 positivity ($p < .001$) (Figures 1–4). The relationships between degree of MnDPDP enhancement and positivities of biliary markers are shown in Table 3. CK7 was positive in 12 HCCs (31.6%) and CK19 was positive in 7 HCCs (18.4%). The correlation between the degree of MnDPDP enhancement and CK7 or CK19 positivity was not significantly positive or negative.

Table 2. Relationship between the degree of MnDPDP enhancement and the Hep Par 1 positivity of HCCs.

MnDPDP enhancement	Hep Par 1			
	(-)	(+)	(++)	(+++)
No	3	1		
Minimal	1	3	4	
Moderate	1	1	3	6
Strong	1	1		13

Table 3. Relationship between the degree of MnDPDP enhancement and the CK7/CK19 positivity of HCCs.

MnDPDP enhancement	CK7 or CK19			
	(-)	(+)	(++)	(+++)
No	4			
Minimal	3	2	2	1
Moderate	7	0	2	2
Strong	10	1	2	2

6. The histologic grades, cell density ratio and Hep Par 1 positivity

The relationships between the histopathologic factors are shown in Table 4, Figure 6 and Figure 7. There were no significant correlations between Hep Par 1 positivity and the histologic grades, the histologic grades and cell density ratio, or Hep Par 1 positivity and cell density ratio.

Table 4. Relationship between Hep Par 1 positivity and histologic grade of HCC.

Hep Par 1	Histologic Grade				
	G I+II	G II	G II+III	G III	G III+IV
(-)		2	1	2	1
(+)	1	3	1	1	
(++)		3	2	3	1
(+++)	1	9	4	2	1

Figure 6. Relationship between histologic grade and the tumor to non-tumor cell density ratio.

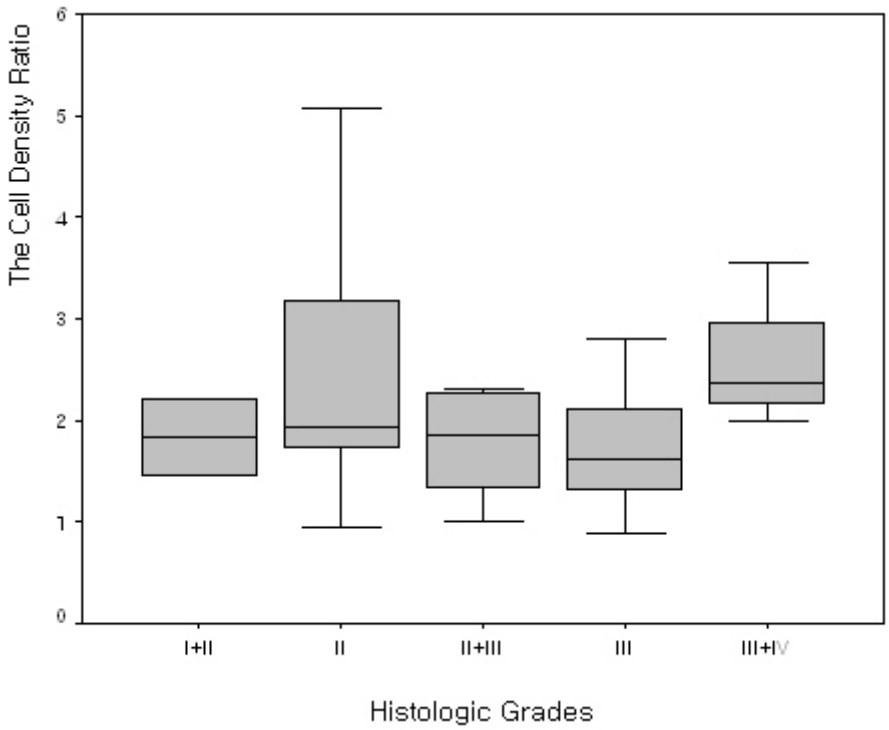

Figure 7. Relationship between Hep Par 1 positivity and the tumor to non-tumor cell density ratio.

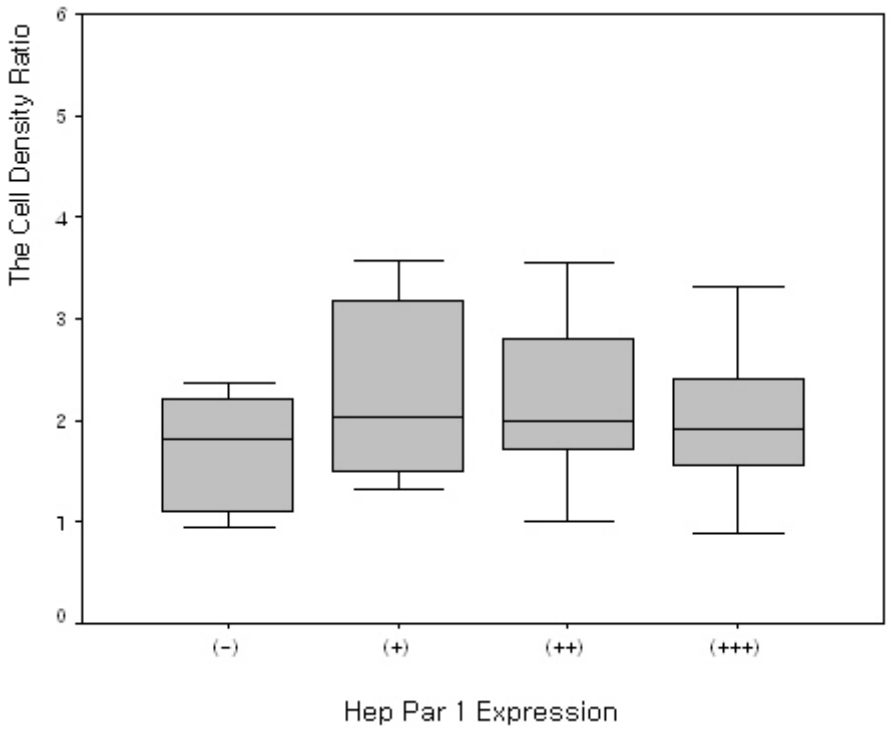

IV. Discussions

MnDPDP is a manganese chelate derived from vitamin B6. Its full chemical name is Mn (II)-N,N'-dipyridoxalethylenediamine-N,N'-diacetate-5,5'-bis(phosphate) and its molecular formula is $Cl_2H_{27}MnN_4Na_3O_{14}P_2$. The active ingredient in MnDPDP is Mn dipyridoxyl diphosphate, a metal chelate of Mn with two linked pyridoxal 5'-phosphate groups. The ligand pyridoxal 5'-phosphate is a catalytically active form of vitamin B6. The mechanisms of the intracellular uptake of MnDPDP in the liver still remain unknown. Initially, it was suggested that MnDPDP associated with the pyridoxine complex and that uptake was mediated by the pyridoxine transporter, but this assertion was refuted by Gallez et al[15]. Two hypothetical mechanisms of uptake of the complex are following: passive diffusion of free Mn^{++} through the membrane or nonspecific uptake by an anion transporter.

Despite being called a "liver-specific" contrast agents, MnDPDP is not entirely specific to liver cells. Enhancement of other organs such as the pancreas, the renal cortex, and adrenal glands has been observed[16-18], which are known as mitochondria-rich tissues. This may be related to their active functional status and their capacity for manganese uptake. Some authors reported that uptake of MnDPDP might even be seen

in cases of liver metastases from endocrine tumors[19, 20]. These uptakes of MnDPDP could also be explained by the functional status of endocrine cells, which are characterized by the presence of numerous mitochondria.

The relationship between the degree of MnDPDP uptake and the nuclear grades of HCCs has been a controversial issue. In the present study, the MnDPDP uptake into HCCs was variable even in HCCs of the same histologic grades and no correlation could be found. On the other hand, the uptake of MnDPDP was strongly correlated with hepatocyte antibody expression. Hep Par 1 is a monoclonal antibody developed using tissue from a failed formalin-fixed allograft liver[21]. The stain has a characteristically coarse granular quality and is negative in the bile duct and stromal cells. The granular intracytoplasmic staining pattern suggests organelle localization, possibly mitochondrial, but the target antigen remains unknown. It reacts to an as yet unidentified cytoplasmic marker of normal and neoplastic hepatocytes. Initial reports have shown that Hep Par 1 is a highly sensitive and reasonably specific marker of hepatocellular differentiation[21-23]. However, Hep Par 1 expression may be very heterogeneous and is often present in other nonhepatic malignant tumors such as gastrointestinal adenocarinomas, cervix adenocarinomas, malignant melanomas, neuroendocrine tumors and some lung cancers [24-27].

The relationship between Hep Par 1 positivity and HCC differentiation is unclear because approximately 10–20% of HCC cases are reportedly negative for Hep Par 1[28]. Recently, Chu et al[27] reported that the level of Hep expression in HCCs corresponded to the nuclear grades and growth patters: expression in 92% of HCCs, including 100% of nuclear grade 1 and 2 tumors, 84% of nuclear grade 3 tumors, and 50% of nuclear grade 4 tumors. In HCCs with a compact growth pattern, the Hep sensitivity was 81%, whereas the sensitivity was 98% in HCCs with a trabecular, pseudoglandular, or scirrhous growth pattern. In another study by Kumagai et al[29], well-differentiated and trabecular type HCC areas showed stronger positivity of Hep Par 1 than poorly differentiated or undifferentiated areas. In the present study, there were 6 Hep Par 1 negative HCCs and they showed variable nuclear grades and histologic types; there were 2 grade II trabecular HCCs, one grade II+III scirrhous HCC, one grade III trabecular HCC, one grade III mixed HCC, and one grade III+IV compact HCC. The nuclear grades did not correlate with MnDPDP uptake or Hep Par 1 expression in this study.

The mechanisms of MnDPDP uptake and Hep Par 1 expression have some commonalities. First, both are specific to normal hepatocytes and hepatocyte-derived tumors. Second, they are also positive in non-hepatic tumors such as endocrine tumors,

with even lower sensitivity and specificity. Third, mitochondria may play an important role in MnDPDP uptake and Hep Par 1 positivity. At any rate, the clinical significance of Hep Par 1 expression in HCC should be further investigated, at this would expand the clinical role of MnDPDP in HCC cases.

The present study showed that the cellularity reflected by the tumor to non-tumor cell density ratio was also associated with the degree of MnDPDP uptake in the HCCs. Cell density was described by the International Working Party[30] as useful in distinguishing high-grade dysplastic nodules from HCC. In well-differentiated HCC, a marked increase of cell density accompanied by a decreased cell size and an increased nuclear cytoplasm ratio are prominent. Kojiro M[31] observed that the nuclear/cytoplasm ratio increases in well-differentiated HCCs, was almost equal to that of a normal hepatocyte in moderately differentiated HCCs, and then increased again in poorly differentiated HCCs because of reduced cytoplasm. In this study, two peaks of cell density were seen in grade II and grade III+ IV HCCs, and there was a tendency towards high MnDPDP enhancement in grade II HCCs. However, a high nuclear-cytoplasmic ratio with a nuclear density greater than twice the normal density was one of the criteria in favor of HCC, but the cell density itself did not influence the determination of nuclear differentiation within cases of HCCs. Nonetheless, the high

cell density in HCC may reflect rapidly proliferative lesions, even in lesions showing grossly the same nuclear grade. Also, cell density may increases in cases of HCC of the small cell type with progenitor cell features which are relatively poorly differentiated. This will be discussed later.

We investigated the expression of CK7 and CK 19, two markers of biliary differentiation, which are expressed in the bile duct. Osborn et al[32] and Fischer et al[33] have reported that hepatocellular carcinoma cells express CK8 and CK 18, but not CK7 or CK19. However, there have been several reports describing the expression of CK17 and CK19 in hepatocellular carcinoma. HCCs with positive biliary markers showed features of more aggressive disease and poorer prognosis compared with HCCs without biliary markers[34-37]. Recently, hepatic progenitor cells have been reported to be strongly immunoreactive for CK7 and CK19, and intermediate hepatocyte-like cells immunoreactive for CK7[38].

There is increasing evidence that stem cells of the liver and the two major cell types, hepatocytes and biliary epithelial cells, are believed to originate from the same progenitor cells. Since progenitor cells can differentiate into both hepatocytes and biliary epithelial cells, progenitor cells can express both hepatocyte differentiation markers and biliary differentiation markers. Primary liver carcinoma of an intermediate

(hepatocyte-bile duct cell) phenotype, named intermediate carcinoma, has been reported: it consists of small cells with a phenotype intermediate between hepatocytes and cholangiocytes, and simultaneously expresses hepatocyte and biliary markers[39, 40]. A small cell type HCC with progenitor cell features has been also described[40]. The small cell type HCC is predominantly composed of small neoplastic cells with slightly more abundant eosinophilic cytoplasm than in the intermediate carcinomas but less than in typical HCCs. These two kinds of carcinomas which arise from hepatic progenitor cells are composed of small, oval shaped cells with relatively compact cellularity and a high nucleus to cytoplasm ratio[41]. Therefore, it was expected that these carcinomas might influence the degree of MnDPDP enhancement because of their high cellular density. However, immunostaining for Hep Par 1 demonstrated a positive staining of HCC cells while demonstrating a negative staining of small cells, and there were no positive or negative correlations between the degree of MnDPDP enhancement and biliary marker positivity. Therefore, increased cell density caused by small cell features does not seem to result in increased MnDPDP enhancement.

This study has limitations. First, complete slice by slice pathologic-imaging matching was not technically feasible. Thus, varieties of histopathologic characteristics in a single tumor nodule could not be evaluated and so the most representative

characteristics of each tumor were used. Second, despite the best efforts to include a wide variety of HCC histopathologic types, it was not feasible to include all growth and cell types and both ends of the nuclear grade. However, the histopathologic types included a range of surgically proven materials sufficiently large to produce results with statistical significance.

V. Conclusion

In conclusion, this study shows that the degree of MnDPDP enhancement was strongly correlated with hepatocyte monoclonal antibody expression and tumor to non-tumor cellular density ratio, but it was not related to biliary markers. In this study, no significant correlation was seen between the uptake of MnDPDP and nuclear grade.

V. References

1. Semelka RC, Martin DR, Balci C, Lance T. Focal liver lesions: comparison of dual-phase CT and multisequence multiplanar MR imaging including dynamic gadolinium enhancement. J Magn Reson Imaging 2001;13:397-401.
2. Elizondo G, Fretz CJ, Stark DD, Rocklage SM, Quay SC, Worah D, et al. Preclinical evaluation of MnDPDP: new paramagnetic hepatobiliary contrast agent for MR imaging. Radiology 1991;178:73-78.
3. Balci NC, Semelka RC. Contrast agents for MR imaging of the liver. Radiol Clin North Am 2005;43:887-898.
4. Hamm B, Vogl TJ, Branding G, Schnell B, Taupitz M, Wolf KJ, et al. Focal liver lesions: MR imaging with Mn-DPDP – Initial clinical results in 40 patients. Radiology 1992;182:167-174.
5. Sahani DV, O'Malley ME, Bhat S, Hahn PF, Saini S. Contrast-enhanced MRI of the liver with mangafodipir trisodium: imaging technique and results. J Comput Assist Tomogr 2002;26:216-222.
6. Helmberger TK, Laubenberger J, Rummeny E, Jung G, Sievers K, Dohring W, et al. MRI characteristics in focal hepatic disease before and after administration of MnDPDP: discriminant analysis as a diagnostic tool. Eur Radiol 2002;12:62-70.
7. Kim MJ, Kim JH, Lim JS, Oh YT, Chung JJ, Choi JS, et al. Detection and characterization of focal hepatic lesions: mangafodipir vs. superparamagnetic iron oxide-enhanced magnetic resonance imaging. J Magn Reson Imaging 2004;20:612-621.
8. Rofsky NM, Weinreb JC, Bernardino ME, Young SW, Lee JK, Noz ME. Hepatocellular tumors: characterization with Mn-DPDP-enhanced MR imaging. Radiology

1993;188:53-59.

9. Liou J, Lee JK, Borrello JA, Brown JJ. Differentiation of hepatomas from nonhepatomatous masses: use of MnDPDP-enhanced MR images. Magn Reson Imaging 1994;12:71-79.

10. Coffin CM, Diche T, Mahfouz A, Alexandre M, Caseiro-Alves F, Rahmouni A, et al. Benign and malignant hepatocellular tumors: evaluation of tumoral enhancement after mangafodipir trisodium injection on MR imaging. Eur Radiol 1999;9:444-449.

11. Oudkerk M, Torres CG, Song B, Konig M, Grimm J, Fernandez-Cuadrado J, et al. Characterization of liver lesions with mangafodipir trisodium-enhanced MR imaging: multicenter study comparing MR and dual-phase spiral CT. Radiology 2002;223:517-524.

12. Ni Y, Marchal G, Zhang X, Van Hecke P, Michiels J, Yu J, et al. The uptake of manganese dipyridoxal-diphosphate by chemically induced hepatocellular carcinoma in rats. A correlation between contrast-media-enhanced magnetic resonance imaging, tumor differentiation, and vascularization. Invest Radiol 1993;28:520-528.

13. Murakami T, Baron RL, Peterson MS, Oliver JH 3rd, Davis PL, Confer SR, et al. Hepatocellular carcinoma: MR imaging with mangafodipir trisodium (Mn-DPDP). Radiology 1996;200:69-77.

14. Scharitzer M, Schima W, Schober E, Reimer P, Helmberger TK, Holzknecht N, et al. Characterization of hepatocellular tumors: value of mangafodipir-enhanced magnetic resonance imaging. J Comput Assist Tomogr 2005;29:181-190.

15. Gallez B, Baudelet C, Adline J, Charbon V, Lambert DM. The uptake of Mn-DPDP by hepatocytes is not mediated by the facilitated transport of pyridoxine. Magn Reson Imaging 1996;14:1191-1195.

16. Wang, C. Mangafodipir trisodium (MnDPDP)-enhanced magnetic resonance imaging of the liver and pancreas. Acta Radiol Suppl 1998;415:1-31.

17. Mitchell DG, Outwater EK, Matteucci T, Rubin DL, Chezmar JL, Saini S. Adrenal gland enhancement at MR imaging with Mn-DPDP. Radiology, 1995 194:783-787.

18. Hustvedt SO, Grant D, Southon TE, Zech K. Plasma pharmacokinetics, tissue distribution and excretion of MnDPDP in the rat and dog after intravenous administration. Acta Radiol 1997;38:690-699.

19. Wang C, Ahlstrom H, Eriksson B, Lonnemark M, McGill S, Hemmingsson A. Uptake of mangafodipir trisodium in liver metastases from endocrine tumors. J Magn Reson Imaging 1998;8:682-686.

20. Mathieu D, Coffin C, Kobeiter H, Caseiro-Alves F, Mahfouz A, Rahmouni A, et al. Unexpected MR-T1 enhancement of endocrine liver metastases with mangafodipir. J Magn Reson Imaging 1999;10:193-195.

21. Wennerberg AE, Nalesnik MA, Coleman WB. Hepatocyte paraffin 1: a monoclonal antibody that reacts with hepatocytes and can be used for differential diagnosis of hepatic tumors. Am J Pathol 1993;143:1050-1054.

22. Leong AS, Sormunen RT, Tsui WM, Liew CT. Hep Par 1 and selected antibodies in the immunohistological distinction of hepatocellular carcinoma from cholangiocarcinoma, combined tumours and metastatic carcinoma. Histopathology 1998;33:318-324.

23. Zimmerman RL, Burke MA, Young NA, Solomides CC, Bibbo M. Diagnostic value of hepatocyte paraffin 1 antibody to discriminate hepatocellular carcinoma from metastatic carcinoma in fine-needle aspiration biopsies of the liver. Cancer 2001;93:288-291.

24. Lugli A, Tornillo L, Mirlacher M, Bundi M, Sauter G, Terracciano LM. Hepatocyte paraffin 1 expression in human normal and neoplastic tissues: tissue microarray analysis

on 3,940 tissue samples. Am J Clin Pathol 2004;122:721-727.

25. Villari D, Caruso R, Grosso M, Vitarelli E, Righi M, Barresi G. Hep Par 1 in gastric and bowel carcinomas: an immunohistochemical study. Pathology 2002;34:423-426.

26. Fan Z, van de Rijn M, Montgomery K, Rouse RV. Hep par 1 antibody stain for the differential diagnosis of hepatocellular carcinoma: 676 tumors tested using tissue microarrays and conventional tissue sections. Mod Pathol 2003;16:137-144.

27. Chu PG, Ishizawa S, Wu E, Weiss LM. Hepatocyte antigen as a marker of hepatocellular carcinoma: an immunohistochemical comparison to carcinoembryonic antigen, CD10, and alpha-fetoprotein. Am J Surg Pathol 2002;26:978-988.

28. Minervini MI, Demetris AJ, Lee RG, Carr BI, Madariaga J, Nalesnik MA. Utilization of hepatocyte-specific antibody in the immunocytochemical evaluation of liver tumors. Mod Pathol 1997;10:686-692.

29. Kumagai I, Masuda T, Sato S, Ishikawa K. Immunoreactivity to monoclonal antibody, Hep Par 1, in human hepatocellular carcinomas according to histopathological grade and histological pattern. Hepatol Res 2001;20:312-319.

30. Terminology of nodular hepatocellular lesions. International Working Party. Hepatology 1995;22:983-993.

31. Kojiro M. Histopathology of liver cancers. Best Pract Res Clin Gastroenterol 2005;19:39-62.

32. Osborn M, van Lessen G, Weber K, Kloppel G, Altmannsberger M. Differential diagnosis of gastrointestinal carcinomas by using monoclonal antibodies specific for individual keratin polypeptides. Lab Invest 1986;55:497-504.

33. Fischer HP, Altmannsberger M, Weber K, Osborn M. Keratin polypeptides in malignant epithelial liver tumors. Differential diagnostic and histogenetic aspects. Am J Pathol

1987;127:530-537.

34. Van Eyken P, Sciot R, Paterson A, Callea F, Kew MC, Desmet VJ. Cytokeratin expression in hepatocellular carcinoma: an immunohistochemical study. Hum Pathol 1988;19:562-568.

35. Wu PC, Fang JW, Lau VK, Lai CL, Lo CK, Lau JY. Classification of hepatocellular carcinoma according to hepatocellular and biliary differentiation markers. Clinical and biological implications. Am J Pathol 1996;149:1167-1175.

36. Uenishi T, Kubo S, Yamamoto T, Shuto T, Ogawa M, Tanaka H, et al. Cytokeratin 19 expression in hepatocellular carcinoma predicts early postoperative recurrence. Cancer Sci 2003;94:851-857.

37. Ding SJ, Li Y, Tan YX, Jiang MR, Tian B, Liu YK, et al. From proteomic analysis to clinical significance: overexpression of cytokeratin 19 correlates with hepatocellular carcinoma metastasis. Mol Cell Proteomics 2004;3:73-81.

38. Libbrecht L, Roskams T. Hepatic progenitor cells in human liver diseases. Semin Cell Dev Biol 2002;13:389-396.

39. Robrechts C, De Vos R, Van den Heuvel M, Van Cutsem E, Van Damme B, Desmet V, et al. Primary liver tumour of intermediate (hepatocyte-bile duct cell) phenotype: a progenitor cell tumour? Liver 1998;18:288-293.

40. Kim H, Park C, Han KH, Choi J, Kim YB, Kim JK, et al. Primary liver carcinoma of intermediate (hepatocyte-cholangiocyte) phenotype. J Hepatol 2004;40:298-304.

41. Xiao JC, Jin XL, Ruck P, Adam A, Kaiserling E. Hepatic progenitor cells in human liver cirrhosis: immunohistochemical, electron microscopic and immunofluorencence confocal microscopic findings. World J Gastroenterol 2004;10:1208-1211.

ABSTRACT (in Korean)

간세포암의 Mangafodipir trisodium 조영증강 자기공명 영상: 병리학적 특징과의 비교

지도교수 김 명 진

연세대학교 대학원 의학과

김 주 희

Mangafodipir disodium (MnDPDP)는 간세포 특이 조영제로서, 정상 간세포뿐 아니라 종양 간세포에도 섭취되어, 간세포기원 종양의 감별에 이용되고 있다. 이러한 MnDPDP을 이용한 자기공명 영상에서는 간세포암에 다양한 조영증강을 보이고 있는데, 이러한 차이를 보이는 병리학적 특성이 아직 밝혀지지 않았다. 본 연구의 목적은 간세포암종의 자기공명 영상에서 MnDPDP의 섭취 정도와 관련 있는 조직병리학적 요인을 알아보고자 하였다.

수술전에 MnDPDP 조영증강 MRI를 시행한 37명의 38개 간세포암을 대상으로 하였다. 이들에서 조영전 및 MnDPDP 주입하고 15-30분 후에 동위상 및 탈위상의 경사에코영상을 획득하였다. 조영증강 정도의 주관적 rating, MnDPDP 조영증강 전후

의 병변-간의 신호대잡음비, 신호 조영증강비 (%) 등을 조직병리학적 인자, 즉 핵분화도, 종양크기, 성장 유형, 조직학적 유형, 세포 유형, 종양 대 주변조직의 세포밀도비 (세포조밀도) 및 단일클론 간세포항체 (Hep Par 1), 싸이토케라틴 7 (CK7), 싸이토케라틴 19 (CK19) 등의 면역염색 양성비율 등과 비교하였다.

조영전 자기공명영상과 비교하여 MnDPDP 자기공명영상에서는, 간세포암의 평균 신호강도가 59.6에서 95.0 (조영증강비 = 59.5%)로 증가하였고, 간실질은 평균 75.1에서 108.7 (조영증강비 = 45.2%)로 증가하였다. 35개의 간세포암 중, 8개에서 약한 조영증강을, 11개에서 중등도의 조영증강을, 15개에서 강한 조영증강을 보였다. 나머지 4개의 간세포암에서는 육안적으로 식별가능한 정도의 조영증강이 없었다 (10.3%). MnDPDP 조영증강이 증가함에 따라 세포밀도비도 증가하였다 ($p < 0.05$). 또한 MnDPDPD 조영증강 정도와 Hep Par 1 양성도 간에 강한 연관성이 있었다 ($p < 0.001$). MnDPDP 조영증강 정도와 세포분화도, 크기, 성장 유형, 피막의 존재유무, 조직학적 유형, CK7 및 CK19과는 연관관계가 없었다.

결론적으로 간세포암의 초기지연 섭취는 간세포항체 표현 및 세포밀도와 관련이 있었다. 간세포암의 조직학적 분화도는 MnDPDP 조영증강 정도와 직접적인 연관성이 없었다.

핵심되는 말: **간세포암, 자기공명 영상, 자기공명 조영제**